Ultrafast Study of the Photodissociation of Bromoiodomethane in Acetonitrile upon 266 nm Excitation

Alexander N. Tarnovsky, Magnus Wall, Magnus Gustafsson,† Noelle Lascoux, Villy Sundström, and Eva Åkesson*

Department of Chemical Physics, Lund University, Box 124, SE-221 00 Lund, Sweden

Received: November 26, 2001; In Final Form: March 19, 2002

We studied the A-band photodissociation of bromoiodomethane, CH_2BrI, in acetonitrile solution at room temperature by femtosecond pump−probe spectroscopy. Initiated by the 266 nm light, this reaction leads to the CH_2Br-I isomer, most likely produced via in-cage recombination of the CH_2Br and I photofragments. The isomer is formed vibrationally excited with a time constant of ∼7.5 ps and the hottest isomer molecules are observed as early as 1 ps after the UV excitation. Vibrational relaxation of the isomer molecules takes place on two distinct time scales of a few and ∼40 ps. The ground-state lifetime of the isomer is about 2.5 ns.

I. Introduction

For molecules larger than diatomics, a solvent may influence photochemical bond-breaking giving rise to cage-induced isomerization, in which the photofragments caged by the solvent molecules recombine in a configuration different from that of the parent. The dynamics of in-cage isomerization reactions have been of major interest, and molecules such as ICN, OClO may serve as examples.[1,2] UV excitation of CH_2I_2 and CH_2ClI in solution leads to in-cage reaction of the nascent radicals and I atoms yielding the isomers CH_2I-I and CH_2Cl-I as shown in the femtosecond pump−probe,[3,4] and transient resonance Raman studies.[5−7] The appearance of the isomers in the pump−probe experiments is manifested by their two-band structured absorption, a strong and a weaker band, located in the visible spectral region.[3,4] DFT calculations confirmed that the CH_2I-I and CH_2Cl-I isomers are responsible at least for the strong absorption bands.[5,7] The formation of the CH_2Cl-I and CH_2I-I isomers was also observed earlier upon UV-photolysis of the corresponding dihalomethane in solid Ar- and N_2-matrixes at 12 K.[8,9]

In this study our interest is devoted to the liquid-phase photodissociation of bromoiodomethane, CH_2BrI, that belongs to the dihalomethane series with the general structure CH_2XI (X = F, Cl, Br, I). CH_2BrI has been a famous prototype of a two-chromophore system and for bond-selective photochemistry in gas-phase molecular beam studies.[10−12] It was demonstrated that a preferential C−I bond breaking over C−Br bond breaking and vice versa in CH_2BrI could be achieved by localizing electronic excitation within either the A- or B-band absorptions,[11,12] which are assigned to the n(I)-σ^*(C−I) and n(Br)-σ^*(C−Br) transitions, respectively.[10,12] A-band dissociation in the gas phase is believed to take place on a fully repulsive excited-state surface and the excited CH_2BrI molecule dissociates rapidly compared to molecular rotation,[10,12] forming the CH_2Br radical and the iodine atom in the ground-state $I(^2P_{3/2})$ or spin−orbit excited-state $I^*(^2P_{1/2})$.[12] In matrix isolation experiments similar to the ones performed on CH_2I_2 and CH_2ClI, the CH_2Br-I isomer was observed upon irradiation of bromoiodomethane with monochromatic light corresponding to the long-wavelength part of its absorption spectrum.[8,9] The suggested mechanism for isomer production involved initial formation of the bromomethyl−iodine radical pair from photoexcited CH_2BrI.[8,9] Our femtosecond transient absorption study of CH_2BrI in acetonitrile at 266 nm excitation suggested formation of CH_2Br-I.[13] The nanosecond transient Raman spectra of a solution of CH_2BrI in cyclohexane upon A-band and B-band excitation at 252.8, 239.5, and 217.8 nm were reported, indicating efficient formation of a product species, which was assigned to the CH_2I-Br isomer.[14] It was proposed that both CH_2I-Br and CH_2Br-I isomers may initially be produced, but the more stable CH_2I-Br isomer has a longer lifetime and therefore may be the only species observable on a nanosecond time scale.[14,15] This intriguing behavior of bromoiodomethane in photolyzed liquid solution stimulated our interest to further explore the photodissociation dynamics of this molecule. In this work, we present the femtosecond pump−probe study of the photochemical dynamics of bromoiodomethane in room-temperature acetonitrile solution following A-band photoexcitation. We report the formation of the CH_2Br-I isomer of CH_2BrI and conclude that a cage of acetonitrile molecules confines the I and CH_2Br photofragments giving rise to CH_2Br-I, i.e., similarly to isomerization of the dihalomethanes CH_2I_2 and CH_2ClI. Our results give no support for formation of the second isomer (CH_2I-Br) of bromoiodomethane at our experimental conditions.

II. Experiment

Our femtosecond spectrometer is based on an amplified Ti:Sapphire laser/regenerative amplifier system. The amplified output at 800 nm, ∼0.9 mJ per pulse, 100 fs pulse duration, 1 kHz repetition rate, was split into two beams to generate the 266 nm pump light in a frequency tripler and probe light, which was either a quasi-monochromatic light (300−1200 nm) produced via an OPA or a white-light continuum (330−1000 nm). More details can be found in ref 16. Pump and probe beams were overlapped in the sample at an angle of 10° between the

* Author to whom correspondence should be addressed. E-mail: Eva.Akesson@chemphys.lu.se.

† Department of Organic Chemistry 1, Lund University, Box 124, SE-221 00 Lund, Sweden.

10.1021/jp014306j CCC: $22.00
Published on Web 05/30/2002

beams, and the beam diameters were 180 and 100 μm. The typical pump pulse energy at the sample position was 5 μJ. The method of data acquisition was described previously.[17] Briefly, before interaction with the sample, the analyzing light was split into reference beam and probe beam, the latter was spatially overlapped with the pump beam in the sample. After passing the sample and a monochromator/spectrograph, the reference and probe beams were registered on separate photodiodes (for measurements of kinetic traces at a single probe wavelength) or diode arrays (for measurements of transient spectra). The diode array detection enables us to accumulate simultaneously the kinetics within 274 or 137 nm spectral intervals depending on the employed monochromator gratings. The presented time-resolved spectra in the spectral range 300−940 nm were constructed from the diode array spectra recorded in several such spectral intervals and kinetics recorded at single probe wavelengths between 300 and 380 nm. All measurements were performed at magic angle polarization conditions and at 21 °C.

The sample was circulated through a specially designed Spectrosil quartz flow cell (0.2 or 0.5 mm path length) with a 150 μm thin front window. When measuring the kinetics at a single probe wavelength the sample was a 110 μm thick flowing jet. Signals arising from solvent and the front window were measured when flowing neat acetonitrile and when substituting the sample with a Spectrosil quartz plate matching the front window without disturbing the alignment of the setup. Both solvent and front window signals occurring within ∼500 fs around time-zero with a typical cross-phase modulation appearance[18,19] were substantially smaller compared to the solute signal and were subtracted from the sample signal, either directly (front window signal) or after scaling because of reduction of pump pulse energy due to solute absorption (acetonitrile signal). The Gaussian-shaped apparatus response function (210 fs fwhm) and time zero were measured by using two-photon absorption of neat methanol at the same experimental conditions as used for measuring the sample.[16,20] Alternatively, time zero at different probe wavelengths was obtained by using the nonresonant pump−probe signals from pure acetonitrile or the Spectrosil quartz plate.[18] All data were corrected for chirp in the probe light. To fit the kinetic traces, we used the software package Spectra-Solve version 1.5 and the kinetics were convoluted with the apparatus response function centered at zero time delay between pump and probe pulses. Positive ΔA signal corresponds to pump-induced increase in the sample absorption compared to unexcited sample. CH_2BrI (∼94% pure) was synthesized as described in ref 21. Acetonitrile (Merck, p.a.) was used without further purification.

III. Results and Discussion

The measured UV absorption spectrum of CH_2BrI in acetonitrile solution is shown in Figure 1. The spectrum exhibits the two broad A- and B-bands at 263 nm and at 212 nm due to the n(I)-σ*(C−I) and n(Br)-σ*(C−Br) transitions, respectively, and an intense peak at shorter wavelengths due to Rydberg transitions on the I atom.[10,12] These spectral features are the same as for the absorption spectra of CH_2BrI in cyclohexane and in the gas-phase known from literature.[12,22,23] The absorption spectra demonstrate a lack of vibrational structure suggesting the photodissociation reactions in the excited states associated with A- and B-bands may occur faster than recurrent vibrational motion along Franck−Condon active coordinates in the gas phase as well as in solution. By analogy with CH_3Br and CH_3I, each of the A- and B-bands of CH_2BrI was considered to represent three electronic transitions from the ground state to

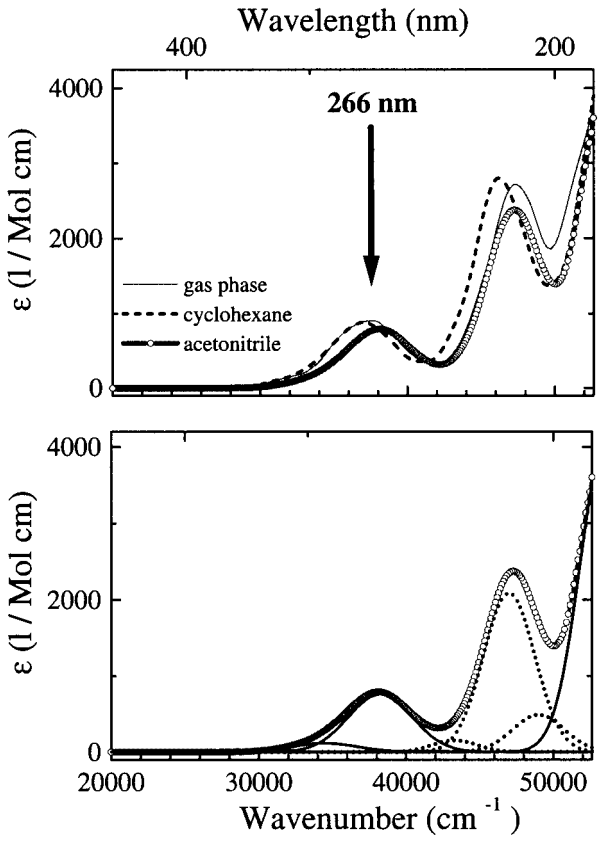

Figure 1. Top panel: Steady-state absorption spectra of bromoiodomethane in the gas phase, ref 22, and in cyclohexane and acetonitrile. Bottom panel: The absorption spectrum of bromoiodomethane in acetonitrile is deconvoluted into a sum of six Gaussian functions with each three of them representing the ground state-Q transitions n(I)-σ*(C−I) (lines) and n(Br)-σ*(C−Br) (dotted). The result of such deconvolution is shown.

the so-called Q excited states with energies increasing in the order of $^3Q_1$, $^3Q_0$, $^1Q_1$ and localized on the C−I (n(I)-σ*(C−I)) and C−Br (n(Br)-σ*(C−Br)) chromophores.[22] We fitted the spectrum to a sum of six Gaussian functions taken to represent the ground-state Q-transitions and found the resulting Gaussians centered at 34450, 38240, 40990 cm^{-1} for the n(I)-σ*(C−I) transition, and at 43310, 47000, 49000 cm^{-1} for the n(Br)-σ*-(C−Br) transition. Although being qualitative, this result enabled us to estimate the spectral overlap between the 266 nm pump and the absorption B-band, and is in agreement with the previously published deconvolution of CH_2BrI spectrum in cyclohexane.[22] Photodissociation studies of CH_2BrI in the gas and liquid phases suggest that the molecules must be excited to the B-band absorption to cause breaking of the C−Br bond.[10,12,22] Excitation at 266 nm is located on the C−I chromophore and is unlikely to overlap the lowest energy subband of the B-band absorption. Therefore, the dominant dissociation pathway in this study is C−I bond breaking in photoexcited bromoiodomethane, CH_2BrI^*. Three competitive reactions are expected to follow:

formation of isomer:

$$CH_2BrI^* \rightarrow CH_2Br + [I(^2P_{3/2}) \text{ or } I^*(^2P_{1/2})] \text{ in-cage} \rightarrow CH_2Br\text{-}I \quad (1)$$

recombination into parent:

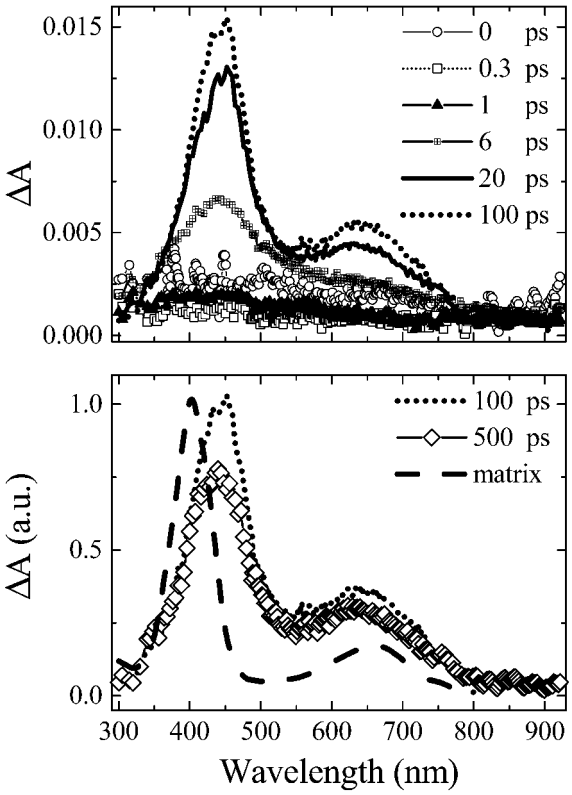

Figure 2. Top panel: Measured transient absorption spectra of CH_2BrI (30 mM) in CH_3CN. The time delays between the 266 nm pump pulses and the probe pulses are given in the inserts of the top and bottom panels. Below 360 nm, the transient absorption spectra are constructed from kinetics measured at single wavelengths in the 110 μm thick jet and scaled to the main spectrum measured in the flow cell of 0.5 mm path length. Bottom panel: Measured transient absorption spectrum at 100 ps (dotted line) same as shown in top panel and the spectrum at the delay 500 ps (symbols) normalized at the blue maximum of the 100 ps spectrum. For comparison, the spectrum of the CH_2Br-I isomer (dashed line) in N_2 matrix at 12 K normalized at the blue peak is shown, refs 8, 9.

$$CH_2BrI^* \rightarrow CH_2Br + [I(^2P_{3/2}) \text{ or } I^*(^2P_{1/2})] \text{ in-cage} \rightarrow CH_2BrI \quad (2)$$

and cage escape:

$$CH_2BrI^* \rightarrow CH_2Br + [I(^2P_{3/2}) \text{ or } I^*(^2P_{1/2})] \text{ in-cage} \rightarrow CH_2Br_{solvated} + I \text{ (or } I^*)_{solvated} \quad (3)$$

We have measured the time-resolved spectra between 300 and 940 nm and kinetics at several probing wavelengths from 300 to 1200 nm to identify the processes that occur following the bromoiodomethane photodissociation and the nature of the reaction products. The measured spectra and kinetics are summarized in Figures 2−4. A summary of the best fits of the kinetic pump−probe data is given in Table 1. At early time, the dynamics are dominated by a positive signal with an instantaneous rise and a fast decay observed within the whole probe range but more pronounced between 300 and 500 nm. In the kinetics, this signal appears as a slightly asymmetric peak toward positive times and in the time-resolved spectra as a rise and drop of the transient absorption signal between −100 and 200 fs, see Figures 2 and 3. These early time transients can be fitted by an instantaneous rise of the absorption and a fast sub-100 fs decay. The rise below 380 nm is followed by a somewhat longer (∼100 fs) decay. Following this initial fast phase, there

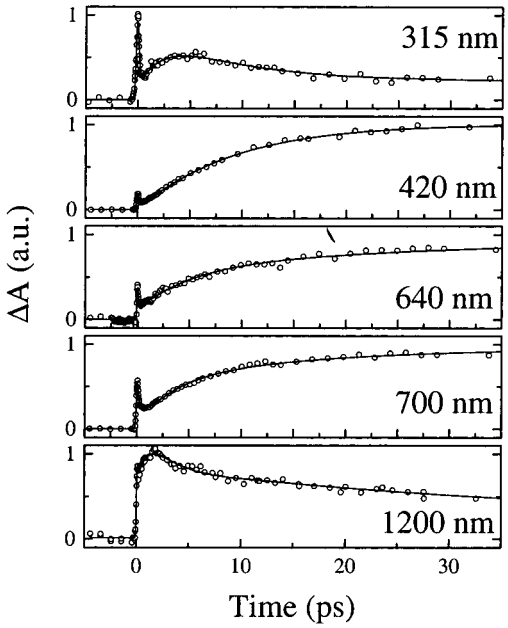

Figure 3. Measured transient absorption kinetics of CH_2BrI (flow jet) in CH_3CN following excitation at 266 nm. The induced absorption (symbols) and fits (lines) are shown for the spectral region 315−1220 nm, the probe wavelengths (nm) are given beside each kinetic curve.

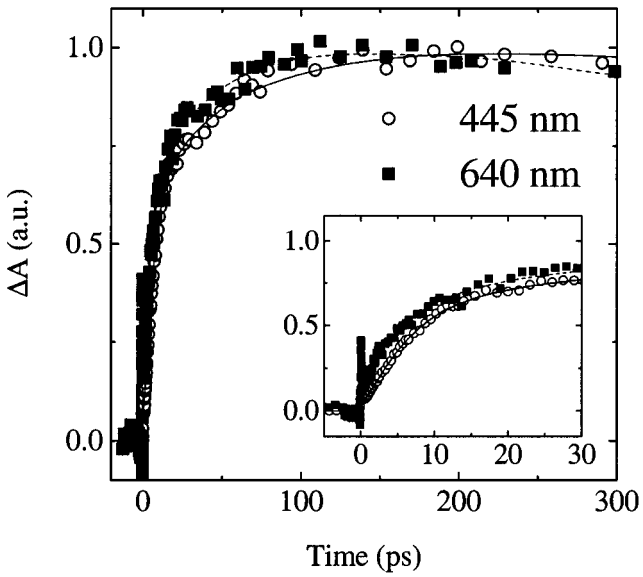

Figure 4. Measured transient absorption kinetics of CH_2BrI (30 mM) in CH_3CN at the probe wavelengths 445 (○) and 640 nm (■) following excitation at 266 nm. The kinetics are normalized to unity at the long-time signal level. The fits to the 445 nm kinetics (dashed line) and to the 640 nm kinetics (solid line) are shown. The measurement at 445 nm was performed in the jet and the one at 640 nm in a 0.5 mm path length flow cell. The inset shows the first 30 ps of the kinetics. For the 640 nm trace, the signal around zero time has contributions from the flow cell window and the solvent.

is a broad and structureless transient absorption signal extending from the ultraviolet to the near-infrared, which further decays with a time constant of 350−650 fs depending on the probe wavelength. At longer times, kinetics exhibit wavelength-dependent time constants of a few picoseconds (1−8 ps) and tens of picoseconds (30−50 ps). The transient spectra in Figure 2 reveal that the few picosecond component is associated with growth of a broad transient absorption and its sharpening into two absorption bands in the visible spectral region. One strong band is centered at 442 nm and a second, weaker, at 632 nm

TABLE 1: Summary of the Best Fits of the Kinetic Pump−Probe Data of CH_2BrI in Acetonitrile[a]

					rise		decay				
λ^b (nm)	A_1 (%)	τ_1 (fs)	A_2 (%)	τ_2 (ps)	A_{3r} (%)	τ_{3r} (ps)	A_{3d} (%)	τ_{3d} (ps)	A_4 (%)	τ_4 (ps)	$A_5{}^c$ (%)
300	52^{+14}_{-24}	160 ± 50	26^{+29}_{-16}	0.5 ± 0.1	-42 ± 19	1.1 ± 0.3	14 ± 8	5.5 ± 0.8	4 ± 3	28 ± 5	4 ± 1
315	28 ± 15	120 ± 50			-68 ± 16	2.7 ± 0.2	53 ± 11	5.5 ± 1.0	19^{+26}_{-11}	41 ± 8	19^{+28}_{-8}
350	*d*	*d*	11 ± 5	0.24 ± 0.06	-60 ± 42	3.0 ± 0.7	40 ± 9	7.7 ± 1.6	-35 ± 12	51 ± 8	49 ± 22
380	24^{+17}_{-5}	56 ± 10			-44 ± 18	3.6 ± 0.4			-23 ± 4	69^{+13}_{-16}	76 ± 3
420	*d*	*d*	11 ± 3	0.59 ± 0.17	-81 ± 16	8.8 ± 0.2			-6^{+5}_{-11}	46 ± 3	89 ± 3
445	*d*	*d*	11 ± 7	0.61 ± 0.21	-47 ± 14	6.0 ± 1.1			-45 ± 17	60^{+13}_{-4}	89 ± 7
480	*d*	*d*			-67 ± 6	6.2 ± 0.4			-25 ± 8	49^{+30}_{-19}	100
550	*d*	*d*			-79 ± 2	2.6 ± 0.2			-11 ± 4	45 ± 5	100
600	*d*	*d*	12 ± 8	0.29 ± 0.04	-39 ± 10	2.7 ± 0.4			-46 ± 6	25 ± 3	88 ± 8
640	*d*	*d*	8^{+8}_{-4}	$0.55^{+0.3}_{-0.25}$	-44 ± 5	5.0 ± 0.2			-38 ± 2	42 ± 2	92 ± 1
700	*d*	*d*	22 ± 14	0.62 ± 0.21	-39 ± 6	3.8 ± 0.3			-34 ± 3	21 ± 3	78 ± 5
815	*d*	*d*			-76 ± 23	1.8 ± 0.5	11^{+18}_{-8}	6.2 ± 0.3	27 ± 11	29 ± 7	62 ± 11
870	*d*	*d*	7^{+20}_{-8}	0.46 ± 0.17	-75 ± 11	2.2 ± 0.4	42 ± 11	5.3 ± 1.3	17 ± 10	27 ± 5	34 ± 11
1200	19^{+27}_{-13}	52^{+5}_{-30}			-59 ± 26	1.0 ± 0.3	51 ± 24	1.6 ± 0.3	23 ± 14	40 ± 2	7 ± 4

[a] Instrumental response function width (fwhm) 210 fs (the width was somewhat longer below 315 nm, 270 fs). To fit the kinetics, the function $F(t) = \sum_{i=1}^{5}[A_i \exp(-t/\tau_i)] + A_5$ convoluted with instrumental response function was used. Negative and positive amplitudes represent rise and decay components, respectively. Amplitudes of the decay and rise components are normalized such that ΣA_i of the decay components equals 100%. Errors represent standard deviation from the mean of best-fits parameters for all measurements employed at given wavelength. Unsymmetrical errors are given if best-fit parameters contain outliers and show the degree of asymmetry of a distribution around its mean. [b] Wavelength at which the transient change in optical density was measured. [c] A time constant of 2500 ps was included to represent a change in optical density at long time delays. [d] Wavelength at which a fast-decaying component with a time comparable or shorter than one-fifth of the response function was found. Since in this case the values of τ_1 were too fast to be determined reliably we did not attempt to include the corresponding amplitude into the Table 1.

manifesting the formation of a product species. For probe wavelengths at the absorption peaks (445 and 640 nm) the kinetics are very similar and can be superimposed, Figure 4. At 50 ps, these bands attain equilibrium and up to 200 ps they exhibit negligible change of the spectral shape and amplitude. In the final stage of temporal evolution, the 442 and 632 nm absorption bands decay slowly on a subnanosecond time scale. The decay is accompanied by a very weak increase of the absorption around 340−360 nm and at 315 nm. The same time constant of $2.2.5^{+0.55}_{-0.25}$ ns for the slow decay was evaluated from the kinetics measured at 445, 600, and 640 nm. This suggests that the same species gives rise to the two absorption bands. The kinetic time profile at 445 nm was found to be independent of the CH_2BrI concentration (Figure 5) suggesting that the species decays via a first-order process.

We now turn to the interpretation of the data presented in Figures 2−4. We assign the instantaneous signal rise to population of the electronically excited state (n,σ^*) of the parent molecule, CH_2BrI, by the 266 nm pump. Then, the ultrafast decay of this signal represents the evolution of the population on the excited-state potential energy surface out of the initially excited Franck−Condon region. Sub-100 fs dynamics were also observed upon the A-band photodissociation of CH_2BrI in cyclohexane in resonance Raman experiments and were interpreted as arising from C−I bond lengthening, C−Br bond shortening, increase of the H−C−Br angles, and decrease of I−C−Br angle.[23] Another possibility is that the initially excited state decays very rapidly into the lower-lying excited state similarly to what was proposed for the excited CF_2I_2 molecule (30 fs decay).[24,25] An interpretation assigning the short-time dynamics at all probe wavelengths to the CH_2Br radical is not consistent with the amount of excess vibrational energy stored in the radical immediately after the photodissociation. Since only about 14% of the total available energy in C−I breaking appears as vibrational excitation of the CH_2Br radical[12] we expect that the hot CH_2Br only contributes to the observed early-time dynamics at probe wavelengths shorter than ∼370 nm.[26]

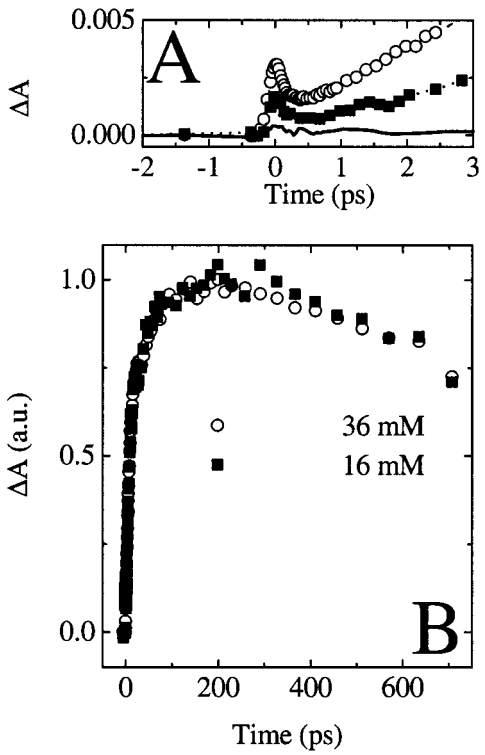

Figure 5. Transient absorption kinetics of CH_2BrI in CH_3CN measured in the flow jet at the pump/probe wavelengths 266/445 nm. The early time (panel A) and full time (panel B) windows of the kinetics are shown. Panel A: The response of neat CH_3CN flowing through the jet is shown by a solid line. The symbols connected by lines represent the CH_2BrI signal at concentrations of 36 (○) and 16 (■) mM. Panel B: Concentration dependence of CH_2BrI kinetics. Superimposed traces in Panel B are the same as in Panel A but normalized at long times (∼200 ps).

The dual absorption band spectrum observed in the present study can be assigned readily to the CH_2Br-I isomer. This is

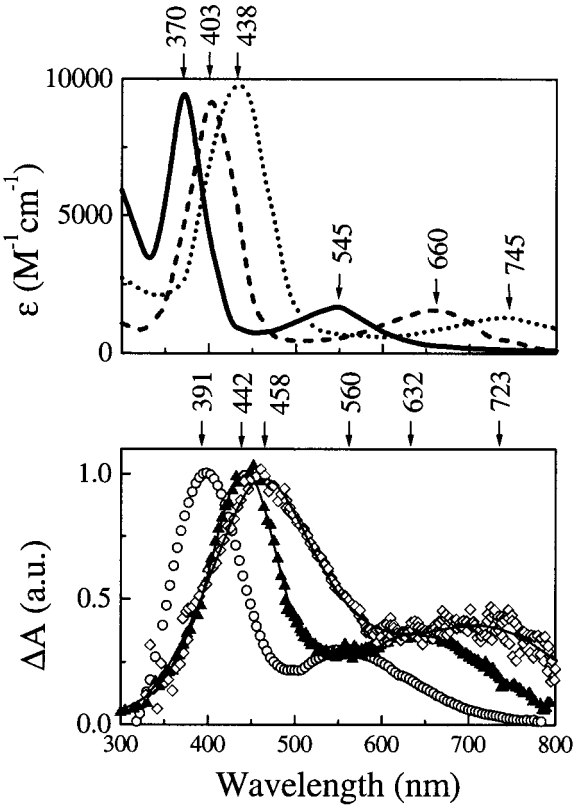

Figure 6. Top panel: The spectra of the isomers CH_2I-I (solid line), CH_2Br-I (dashed line), and CH_2Cl-I (dotted line) in N_2 matrix at 12 K redrawn from the work of Maier et al., refs 8, 9. Bottom panel: The transient absorption spectra of the dihalomethanes CH_2I_2 (open circles), CH_2BrI (solid triangles), and CH_2ClI (open diamonds) obtained in the femtosecond pump−probe experiments. The excitation wavelengths were 266 nm for CH_2BrI and CH_2ClI, and 310 nm for CH_2I_2. Acetonitrile is used as a solvent. The spectra were recorded at the delays 200 ps (CH_2I_2), 100 ps (CH_2BrI), and 50 ps (CH_2ClI) and assigned to the photoisomers CH_2I-I (ref 3), CH_2Br-I (this work), and CH_2Cl-I (ref 4).

evident from comparison between the observed bands and the absorption spectrum of the CH_2Br-I product produced upon UV photolysis of bromoiodomethane embedded in cold matrixes, see Figure 6. The spectra of CH_2Br-I measured in room-temperature acetonitrile solution and cold matrixes agree in the same way as the spectra of CH_2I-I and CH_2Cl-I isomers obtained under similar conditions, Figure 6. The DFT calculations,[14] which predict an intense ground-to-singlet-state transition at 422 nm in the CH_2Br-I species, give further support to our assignment. Our observation that the measurements at the absorption maxima of the blue and the red bands exhibit the same kinetics of formation and decay shows that these bands belong to the same species. This is also supported by the observation that irradiation of low-temperature matrixes with light corresponding to one of the CH_2Br-I absorption bands depleted the absorption in both bands.[8,9]

Alternative assignments for the 442 and 632 nm absorption bands to I atoms, CH_2Br radicals, and hot CH_2BrI parent molecules formed due to primary geminate recombination can be ruled out. Solvated I atoms form a charge-transfer (CT) complex with acetonitrile molecules and their absorption is known to peak at 275 nm.[27] The reddest absorption edge of the CH_2Br radical is located at wavelengths shorter than 335 nm.[28−31] Even though vibrationally hot CH_2BrI is very likely to absorb in the visible, its electronic spectrum will be flat, featureless, and much reduced in strength relative to that of the vibrational cool molecules, not like the observed structured and intense spectrum. In addition, vibrationally hot parent molecules are expected to attain the thermalized absorption spectrum on a picosecond time scale, in sharp contrast with the 2.5 ns lifetime of the 442 and 632 nm bands.

The other isomer form, CH_2I-Br, and molecular cation, CH_2BrI^+, do not qualify either as responsible for the observed 442 and 632 nm bands. The CH_2I-Br isomer is predicted by the DFT calculations to have several electronic transitions below 375 nm,[14] at too short wavelengths to account for our observations. Direct production of CH_2BrI^+ from CH_2BrI can be excluded since the pump photon energy used (4.66 eV) is much less than the ionization potential of CH_2BrI (IP $\sim$ 9.5 eV[32]) and a linear variation of ΔA is observed upon 10-fold decrease of the pump pulse energy. An alternative route of the cation formation was proposed for CH_2I_2, which involves the aggregates of the solute molecules existing prior to excitation.[34] In our recent work on CH_2I_2 and CH_2ClI,[3,4] we have not found any support of preexisting clusters in the solutions of the studied dihalomethanes. Instead, for these molecules, both absorption bands were attributed to isomers CH_2X-I. For bromoiodomethane, the kinetic profile at the blue peak of the product absorption spectrum is found to be independent of the CH_2BrI concentration within 0−700 ps, Figure 5. This rules out that clustering of bromoiodomethane leads to the observed absorption bands following the UV excitation. This leaves the CH_2Br-I isomer as the most plausible candidate for the observed bands.

Next, we discuss the spectral evolution on the picosecond time scale associated with the formation and vibrational relaxation of the CH_2Br-I isomer and show how these two processes can be disentangled and their individual temporal characteristics obtained. First, we discuss the vibrational relaxation of the isomer to which we have attributed the tens of picoseconds spectral evolution and a part of the few picosecond evolution, Table 1. By comparison of the time-resolved spectra and kinetics, Figures 2 and 3, we see that the few tens of picoseconds component appearing as a rise or a decay depending on the probe wavelength is a consequence of narrowing of the two absorption bands. As to the faster few picosecond process, the signal rise is slowest for probe wavelengths at the isomer absorption peaks (6 $\pm$ 1 ps), and becomes faster when probing at the wings of the absorption bands, Table 1. When the probe wavelength is tuned away from the equilibrated long-time spectrum to 870−1200 nm and to 300−380 nm, the kinetics demonstrate an even faster absorption rise followed by a slower decay. For example, at the probe wavelength of 1200 nm, the fastest picosecond rise of 1 ps observed in the present experiments is succeeded by a 1.7 ps decay, while at 870 nm a rise of 1.8 ps is followed by a 6.2 ps decay.

These observations, the faster rise at the wings than at the peak of absorption and spectral narrowing are typical for vibrational relaxation of small molecules in solution.[35−41] The absorption of the hot CH_2Br-I isomers, which lies at energies far from the absorption band of the vibrational ground state (equilibrated spectrum), moves toward the equilibrated spectrum as the isomer vibrationally relaxes. In this view, the further to the red the probe wavelength is with respect to the isomer band maximum, the hotter isomer is monitored. An absorption rise with a time constant of 1 ps at 1200 nm is the earliest observation of the isomer and gives the time scale for the hottest CH_2Br-I isomers formed in our experiments. The presence of isomers at these early times is indicated also by the broad (425−460 nm) transient absorption at 1 ps peaking near 427 nm, close

to the maximum of the equilibrated isomer band. The low intensity of this absorption is due to a relatively small fraction of the isomer vibrational energy distribution occupying the low-lying vibrational states at the isomer ground-state potential bottom at 1 ps. It takes longer time (~6 ps) for the whole isomer population to reach the detection windows of 445 and 640 nm corresponding to the absorption maxima of the cold isomer. Similar times, ~10 ps, were reported for intramolecular energy redistribution of vibrationally excited diiodomethane, CH_2I_2, (two quanta of the C−H stretch vibration) prepared by intense mid-IR-excitation.[42−45] Therefore, it is reasonable to assume that the several picosecond vibrational relaxation dynamics are associated with intramolecular energy redistribution (IVR) in the isomer. The tens of picoseconds component may be attributed to vibrational cooling or a second slow vibrational relaxation channel of the isomer, possibly to a slow intramolecular vibrational energy redistribution involving intermediate energy vibrations in the isomer ground state. Excess vibrationally energy transfer from mid-IR-excited diiodomethane to the polar solvent was observed to take place on a similar time scale.[44,43]

To obtain an accurate value for the formation time of the isomer we applied the conservation rule of the electronic transition dipole strength with time.[46] In the present study, the integrated absorption within the two bands at ~442 nm and ~632 nm was found to increase up to ~20 ps with a time constant of $7.5^{+1.1}_{-0.5}$ ps and stay nearly constant from 50 to 200 ps. This shows that the CH_2Br-I isomer formation time constant is ~7.5 ps provided that the conservation rule is applicable. A more detailed description of this analysis will be published elsewhere.[26] The integrated absorption within both bands has a nearly identical rise further reinforcing our assignment of these bands to the same species. The CH_2Br-I isomer is relatively stable in acetonitrile at room temperature as reflected by the 2.5 ns decay of the isomer absorption. A similar ground-state lifetime of the CH_2Br-I isomer, 2−3 ns, was observed in picosecond transient Raman experiments in cyclohexane.[15]

We suggest that the CH_2Br-I isomer is produced from initially formed CH_2Br and I photofragments via recombination within the solvent cage. As for CH_2I_2 photodissociation, in which the caged CH_2I radical was observed within the time range 350 fs−3 ps,[3] the formed CH_2Br and I are trapped for some time in a cage of acetonitrile molecules. The solvent caging lasts for several picoseconds, much shorter than a secondary diffusive geminate recombination that takes place on a time scale of tens of picoseconds or greater.[47] Our results indicate that it takes about 1 ps for the CH_2Br and I fragments to start recombining at the energy level that corresponds to the highly excited vibrational states of the electronic ground state of the CH_2Br-I isomer. This time is an upper limit since probe wavelengths longer than 1200 nm may monitor even hotter isomers. The major fraction of the CH_2Br-I population is formed on a longer time scale of several picoseconds, very likely, in parallel with vibrational cooling of the nascent radicals. Ab initio calculations suggest that isolated isomers of the dihalomethanes CH_2Cl_2, CH_2Br_2, CH_2ClBr, and CH_2I_2 occupy a shallow minimum on a ground-state potential energy surface.[9,48] It seems that nascent radicals must dissipate a significant part of the energy available for recoil in order to be effectively trapped in an isomer ground-state potential well. Nevertheless, spectral evolution of the isomer absorption indicates that the formed CH_2Br-I isomer in solution is internally excited and houses some vibrational energy that dissipates on two distinct time scales of a few and tens of picosecond. The similar conclusion could be drawn for the CH_2I-I and CH_2Cl-I isomers on the basis of our previously published results.[3,4]

Since the DFT calculations predict spectrally quite separated transitions and similar oscillator strength for the CH_2Br-I and CH_2I-Br species, formation of CH_2I-Br is expected to be observed in this experiment. However, we see no clear evidence that bromoiodomethane excited at 266 nm in acetonitrile produces the CH_2I-Br product. On the basis of the amount of energy absorbed, we have found that about 26% of dissociated CH_2BrI yields the CH_2Br-I isomer after 100 ps.[49] The remaining 74% of the nascent CH_2Br radical and I-atom photofragments at 100 ps are distributed between two other reaction channels, i.e., geminate recombination into the parent molecule and cage escape. To determine the relative importance of these two channels, accurate information about the UV absorption of the CH_2Br-I and CH_2Br species is necessary, but is not available (CH_2Br-I) or controversial (CH_2Br, compare refs 28−31). Currently in progress are ab initio calculations (including spin−orbit coupling) of the transition energies of these species and femtosecond transient absorption measurements with probing below 300 nm, which will be helpful in understanding the relative importance of the geminate recombination into the parent molecule and cage escape channels. The relative importance of these two channels also remains to be seen for CH_2ClI and CH_2I_2. Compared to the quantum efficiency of the isomerization of CH_2BrI into CH_2Br-I, the isomerization of CH_2ClI into CH_2Cl-I is less and CH_2I_2 into CH_2I-I is more efficient at the same experimental conditions (9 and 70%, respectively, ref 50).

IV. Conclusion

Following excitation (266 nm) close to the maximum of the A-band absorption of CH_2BrI in acetonitrile, transient absorption spectra and kinetics were measured in the spectral range 300−1200 nm. The time-resolved spectrum at very early times after excitation is dominated by pump-induced excited-state absorption of electronically excited bromoiodomethane. The hot ground-state photoisomer of CH_2BrI, CH_2Br-I, appears with a characteristic time ~1 ps. Vibrational relaxation of the CH_2Br-I isomer takes place on two distinct time scales of a few and tens of picoseconds. The fast channel of the isomer vibrational relaxation is mixed with a slow increase of isomer concentration, characterized by a time constant of ~7.5 ps. At a delay time of 50 ps, the isomer exhibits the equilibrated absorption spectrum consisting of two characteristic bands, a strong band at 442 nm and, a weaker band at 632 nm. The isomer absorption begins to fade at the subnanosecond delays enabling us to estimate the ground-state lifetime of the CH_2Br-I isomer to ~2.5 ns. Within the time scale of our pump−probe experiments 0−700 ps, we see no clear spectral signature of absorption of the second isomer (CH_2I-Br) of bromoiodomethane indicating that this isomer is not formed at our experimental conditions.

Acknowledgment. The authors thank Dr. B. Nelander and Dr. R. Lindh for many fruitful discussions and Dr. T. Pascher for his help with the diode array measurements. Financial support from the Swedish Natural Science Research Council, Magnus Bergwall Foundation, Crafoord Foundation, and Knut and Alice Wallenberg Foundation is gratefully acknowledged.

References and Notes

(1) Helbing, J.; Chergui, M. *J. Phys. Chem. A* **2000**, *104*, 10293; Helbing, J.; Chergui, M.; Fernandez-Alberti, S.; Echave, J.; Halberstadt, N.; Beswick, J. A. *Phys. Chem. Chem. Phys.* **2000**, *2*, 4131, and references therein.

(2) Thomsen, C. L.; Reid, P. J.; Keiding, S. R. *J. Am. Chem. Soc.* **2000**, *122*, 12795, and references therein.
(3) Tarnovsky, A. N.; Alvarez, J.-L.; Yartsev, A.; Sundström, V.; Åkesson, E. *Chem. Phys. Lett.* **1999**, *312*, 121.
(4) Tarnovsky, A. N.; Wall, M.; Rasmusson, M.; Pascher, T.; Åkesson, E. *J. Chin. Chem. Soc.* **2000**, *47*, 769. Special Issue.
(5) Zheng, X.; Phillips, D. L. *J. Phys. Chem. A* **2000**, *104*, 6880.
(6) Kwok, W. M.; Ma, C.; Parker, A. W.; Phillips, D.; Towrie, M.; Matousek, P.; Phillips, D. L. *J. Chem. Phys.* **2000**, *113*, 7471.
(7) Kwok, W. M.; Ma, C.; Parker, A. W.; Phillips, D.; Towrie, M.; Matousek, P.; Zheng, X.; Phillips, D. L. *J. Chem. Phys.* **2001**, *114*, 7536.
(8) Maier, G.; Reisenauer, H. P. *Angew. Chem., Int. Ed. Engl.* **1986**, *25*, 819.
(9) Maier, G.; Reisenauer, H. P.; Hu, J.; Schaad, L. J.; Hess, B. A., Jr. *J. Am. Chem. Soc.* **1990**, *112*, 5117.
(10) Lee, S. J.; Bersohn, R. *J. Phys. Chem.* **1982**, *86*, 728.
(11) Butler, L. J.; Hintsa E. J.; Lee Y. T. *J. Chem. Phys.* **1986**, *84*, 4104.
(12) Butler, L. J.; Hintsa, E. J.; Shane, S. F.; Lee, Y. T. *J. Chem. Phys.* **1987**, *86*, 2051.
(13) Tarnovsky, A. N.; Wall, M.; Pascher, T.; Sundström, V.; Åkesson, E. In *Photophysics and Photochemistry 2000*; Costa de Estoril, Portugal, October, 19−21, 2000, p 144; Åkesson, E.; Tarnovsky, A. N.; Benkö, G.; Yartsev, A.; Sundström, V. In *Femtochemistry*; De Schryver, F. C., De Feyter, S., Schweitzer, G., Eds.; Wiley-VCH: Weinheim, 2001; Chapter 24.
(14) Zheng, X.; Phillips, D. L. *J. Chem. Phys.* **2000**, *113*, 3194.
(15) Kwok, W. M.; Ma, C.; Phillips, D.; Parker, A. W.; Towrie, M.; Matousek, P.; Phillips, D. L. *Chem. Phys. Lett.* **2001**, *341*, 292.
(16) Rasmusson, M.; Tarnovsky, A. N.; Åkesson, E.; Sundström, V. *Chem. Phys. Lett.* **2001**, *335*, 201.
(17) Åberg, U.; Åkesson, E.; Alvarez, J.-L.; Fedchenia, I.; Sundström, V. *Chem. Phys.* **1994**, *183*, 269.
(18) Kovalenko, S. A.; Dobryakov, A. L.; Ruthmann, J.; Ernsting, N. P. *Phys. Rev. A* **1999**, *59*, 2369.
(19) Ekvall, K.; van der Meulen, P.; Dhollande, C.; Berg, L. E.; Pommeret, S.; Naskrecki, R.; Mialocq, J. C. *J. Appl. Phys.* **2000**, *87*, 2340.
(20) Reuther, A.; Laubereau, A.; Nikogosyan, D. N. *Opt. Commun.* **1997**, *141*, 180.
(21) Miyano, S.; Hashimoto, H. *Bull. Chem. Soc. Jpn.* **1971**, *44*, 2864.
(22) Man, S.-Q.; Kwok, W. M.; Phillips, D. L.; Johnson, A. E. *J. Chem. Phys.* **1996**, *105*, 5842.
(23) Mössinger, J. C.; Shallcross, D. E.; Cox, R. A. *J. Chem. Soc. Faraday Trans.* **1998**, *94*, 1391.
(24) Radloff, W.; Farmanara, P.; Stert, V.; Schreiber, E.; Huber, J. R. *Chem. Phys. Lett.* **1998**, *291*, 173.
(25) Farmanara, P.; Stert, V.; Ritze, H. H.; Radloff, W. *J. Chem. Phys.* **2000**, *113*, 1705.
(26) Tarnovsky, A. N.; Lindh, R.; Wall, M.; Gustafsson, M.; Pascher, T.; Sundström, V.; Åkesson, E. In preparation.
(27) Treinin, A.; Hayon, E. *Int. J. Radiat. Phys. Chem.* **1975**, *7*, 387.
(28) Nielsen, O. J.; Munk, J.; Locke, G.; Wallington T. J. *J. Phys. Chem.* **1991**, *95*, 8714.
(29) Villenave, E.; Lesclaux, R. *Chem. Phys. Lett.* **1995**, *236*, 376.
(30) Chong, C. K.; Zheng, X.; Phillips, D. L. *Chem. Phys. Lett.* **2000**, *328*, 113.
(31) Li, Y.; Francisco, J. S. *J. Chem. Phys.* **2001**, *114*, 2879.
(32) The exact IP value for CH_2BrI is not known; di- and polyhalomethanes have ionization potentials about 9.5−11.5 eV, ref 33.
(33) *CRC Handbook of Chemistry and Physics*, 80th ed.; Lide, D. R., Ed.; CRC Press LLC: Boca Raton, FL, 1999; Section 10.
(34) Saitow, K.; Naitoh, Y.; Tominaga, K.; Yoshihara, K. *Chem. Phys. Lett.* **1996**, *262*, 621.
(35) Owrutsky, J. C.; Raftery, D.; Hochstrasser, R. M. *Annu. Rev. Phys. Chem.* **1994**, *45*, 519.
(36) Thomsen, C. L.; Madsen, D.; Thøgersen, J.; Byberg, J. R.; Keiding, S. R. *J. Chem. Phys.* **1999**, *111*, 703.
(37) Berg, M.; Harris, A. L.; Harris, C. B. *Phys. Rev. Lett.* **1985,** *54*, 951; Harris, A. L.; Berg, M.; Harris, C. B. *J. Chem. Phys.* **1986,** *84*, 788; Harris, A. L.; Brown, J. K.; Harris, C. B. *Annu. Rev. Phys. Chem.* **1988,** *39*, 341.
(38) Banin, U.; Ruhman, S. *J. Chem. Phys.* **1993**, *98*, 4391.
(39) Kühne, T.; Vöhringer, P. *J. Chem. Phys.* **1996**, *105*, 10788.
(40) Kliner, D. A. V.; Alfano, J. C.; Barbara, P. F. *J. Chem. Phys.* **1993**, *98*, 5375.
(41) Pugliano, N.; Gnanakaran, S.; Hochstrasser, R. M. *J. Photochem. Photobiol.* **1996**, *102*, 21; Pugliano, N.; Szarka A. Z.; Gnanakaran, S.; Triechel, M.; Hochstrasser, R. M. *J. Chem. Phys.* **1995**, *103*, 6498.
(42) Graener, H.; Laubereau, A. *Appl. Phys. B* **1982**, *29*, 213.
(43) Bakker, H. J.; Planken, P. C. M.; Lagendijk, A. *J. Chem. Phys.* **1991**, *94*, 6007.
(44) Bingemann, D.; King, A. M.; Crim, F. F. *J. Chem. Phys.* **2000**, *113*, 5018.
(45) Charvat, A.; Aβmann, J.; Abel, B.; Schwarzer, D. *J. Phys. Chem. A* **2001**, *105*, 5071.
(46) Bultmann, T.; Ernsting, N. P. *J. Phys. Chem.* **1996**, *100*, 19417.
(47) Nesbitt, D. J.; Hynes. J. T. *J. Chem. Phys.* **1982**, *77*, 2130.
(48) Glukhovtsev, M. N.; Bach, R. D. *Chem. Phys. Lett.* **1997**, *269*, 145.
(49) We estimated the extinction value for CH_2Br-I in acetonitrile, $\epsilon_{ACN} = 6520 \pm 540$ L/mol cm, at 442 nm using the extinction value in the cold N_2 matrix (10 000 l/Mol cm at the maximum of the blue band of CH_2Br-I, ref 9) and assuming that the transition dipole strength of the band is conserved upon going from the matrix to the solution. Using the following equation for the quantum formation yield of the isomer (Φ): $\Phi = (\Delta A/\epsilon_{ACN})(N_A \times 10^{-3})(Fh\nu(\pi r^2))/E(1 - 10^{-OD})$, where OD = 0.22 is the optical density of the sample (0.2 mm path length flow cell) at 266 nm, $E = 1.3 \times 10^{-6}$ J/pulse is the measured incident pump pulse energy, $F = 1.04$ is the measured pump energy loss due to reflection off the cell front window, $h\nu = 7.466 \times 10^{-19}$ J is a 266 nm photon energy, $r = 9 \times 10^{-3}$ cm is the pump beam radius at the sample, $\Delta A = 0.0071$ is the measured transient absorption signal at the probe wavelength 445 nm and 100 ps delay, $N_A = 6.02 \times 10^{23}$ mol^{-1} is the Avogadro's constant, we estimated Φ to be 26 ± 5%. This estimate of Φ represents the fraction of the excited CH_2BrI molecules that underwent the isomerization into CH_2Br-I. Although performed at long time when the isomer spectrum is thermalized, the value of $\Phi = 26\%$ is reached at ∼25 ps since the isomer formation time determined from the rise of integrated absorption is 7.5 ps.
(50) Tarnovsky, A. N.; Wall, M.; Rasmusson, M.; Sundström V.; Åkesson, E. In *Femtochemistry and Femtobiology. Ultrafast Dynamics in Molecular Science*; Douhal, A., Santamaria, J., Eds.; World Scientific: Singapore, 2002; p 247.